J Solid State Electrochem (2007) 11: 231–239
DOI 10.1007/s10008-005-0093-8

ORIGINAL PAPER

Merlin C. E. Bandeira · Joseph A. Crayston · Norberto S. Gonçalves · Lúcia K. Noda · Andrew Glidle · César V. Franco

Electropolymerization of *trans*-[$RuCl_2(vpy)_4$] complex—EQCM and Raman studies

Received: 5 April 2005 / Revised: 18 November 2005 / Accepted: 23 December 2005 / Published online: 8 March 2005

Abstract The electropolymerization of *trans*-[$RuCl_2(vpy)_4$] (vpy=4-vinylpyridine) on Au or Pt electrodes was studied by cyclic voltammetry, electrochemical quartz crystal microbalance (EQCM) technique, and Raman spectroscopy. Cyclic voltammetry of the monomer at a microelectrode shows the typical Ru(III/II) and Ru (IV/III) waves, together with the vinyl reduction waves at −1.5 and −2.45 V and adsorption wave at −0.8 V. Electrodeposition on EQCM technique performed under potential cycling between −0.9 and −2.0 V revealed that the polymerization proceeded well in advance of the vinyl reduction waves. At potentials more positive than −0.9 V, soluble oligomers were deposited irreversibly on the electrode during the oxidative sweep. The film also showed reversible mass changes due to the oxidation and accompanying ingress of charge-balancing anions and solvent into the film. In contrast, potentiostatic growth of the polymer at −1.6 V was slower because the oligomeric material was lost completely from the electrode. Unreacted vinyl groups were detected by in situ Raman spectroscopy for films grown at −0.7, −0.9, and −1.6 V but were absent when the polymerization was carried out at −2.9 V vs Ag/Ag^+.

Keywords trans-[$RuCl_2(vpy)_4$] · Electropolymerization · Raman spectroscopy

M. C. E. Bandeira (✉)
Depto. de Química,
Universidade Federal de Mato Grosso do Sul,
Av. Senador Filinto Muller 1555, CxP:549,
79070-900 Campo Grande, MS, Brazil
e-mail: merlin@nin.ufms.br

J. A. Crayston
School of Chemistry, University of St. Andrews,
St. Andrews, Fife, Scotland KY169ST, UK

N. S. Gonçalves · L. K. Noda · C. V. Franco
Depto. de Química-CFM, Campus Trindade,
Universidade Federal de Santa Catarina,
88040-900 Florianópolis, SC, Brazil

A. Glidle
Chemistry Department, University of Glasgow,
Glasgow, Scotland G12 8QQ, UK

Introduction

Our research group has synthesized and characterized a series of new electropolymerizable complexes with general formula *trans*-[$RuCl_2(L)_4$] [1, 2]. In particular, *trans*-[$RuCl_2(vpy)_4$] [3] (vpy=4-vinylpyridine), bearing four electropolymerizable groups, is readily polymerized to give adherent electroactive films related to those produced with vinylbypridine and vinylterpyridine ligands [4, 5]. Previous studies have shown that the *trans*-[$RuCl_2(vpy)_4$] complex can be electropolymerized onto different substrates, including inert materials such as Pt and Pd [3], iron alloys [6–8], and stainless steel [9]. Electrocatalysis is the main proposed application for electrodes modified by films formed from transition metal complexes [10–16]. The catalyzing properties of such materials are associated with their molecular nature and availability of electrons originated from the redox reactions of the metallic center. As these are immobilized in the polymeric matrix, they can mediate reactions and promote either catalytic oxidation or reduction of a given species in solution. The choice of reactions that can be catalyzed is based on the standard potential of the modified electrode. Although many studies have reported on the synthesis, characterization [17, 18], and application of transition metal complexes [12, 14, 16, 19], the mechanism of electropolymerization itself has not been fully established [5, 20]. Cyclic voltammetry, electrochemical quartz crystal microbalance (EQCM), and Raman spectroscopy results on the electropolymerization of *trans*-[$RuCl_2(vpy)_4$] on Pt or Au electrodes are presented in this report with particular attention to the effects of the polymerization potential on the characteristics of the film

formed along with the understanding of the main processes involved in the electropolymerization.

Experimental

Reagents and synthesis All reagents, solvents, and electrolyte salts employed in this work were of an analytical grade and most of them were used without any further purification. Only 4-vinylpyridine was distilled before its use in the synthesis of *trans*-$[RuCl_2(vpy)_4]$. Details on the synthesis and characterization of *trans*-$[RuCl_2(vpy)_4]$ can be found elsewhere [3, 21, 22].

Electropolymerization A conventional cell containing a single compartment, a working Pt or Au electrode, a Pt gauze counter electrode, and an Ag/Ag^+ electrode as reference was used. The polymerization solution consisted of 5 mmol dm^{-3} *trans*-$[RuCl_2(vpy)_4]$ and 0.1 mol dm^{-3} $TBAPF_6$ in acetonitrile/dichloromethane (3/2 v/v), deaerated with argon during 10 min. Electropolymerization was carried out by direct application of a polymerization potential for a few seconds and potential cycles (CV) between 0.4 and −2.4 V vs Ag/Ag^+ [3, 6].

Instrumentation The experiments were carried out using an E.G. & G. PAR 273A potentiostat/galvanostat interfaced to a personal computer using a National Instruments GPIB. Data were recorded and analyzed using a PARC *M270* v.4.0 computer program.

EQCM For experiments with the EQCM, electropolymerization was carried out by CV and also at fixed potential. The electropolymerization conditions and solution were those previously specified. The QCM electrode electroactive oscillating area was 0.211 cm^2 (10 MHz AT-cut ICM Lab Monitor crystals, OK, USA) and the sensitivity factor 0.232 Hz cm^2 ng^{-1}. All measurements were carried out using a home-built oscillator and a computer-controlled potentiostat.

Raman spectroscopy Raman spectra were obtained in a Renishaw Raman System 3000 equipped with a CCD, using the 632.8-nm line of a He–Ne laser (Spectra-Physics model 127). The laser was focused onto the electrode surface by means of a microscope (Olympus BH2T). The Raman spectra were the average of three acquisitions, using an integration time of 10 s to cover the whole spectral range. Laser power was set to 3 mW. The electrochemical experiments were performed using a PAR model 263 potentiostat. An Au working electrode was placed in a Teflon holder and mounted in a Teflon cell containing the electrolyte. The reference and counter electrode were Ag and Pt wires, respectively. Electropolymerization was performed as previously described. Four different potentials (−0.7, −0.9, −1.6, and −2.9 V vs Ag/Ag^+) were applied and Raman spectra were obtained at deposition times of 300, 600, and 1,200 s. The working electrode was flushed with acetonitrile before spectra acquisition to remove any residual complex.

Computational methods The optimized structure and vibrational band frequencies of the ligand 4-vinylpyridine were calculated at the Hartree–Fock (HF), using the 6-31G (d,p) basis set. All calculations were carried out using the Gaussian 94 and Gaussian 98 programs (Gaussian) [23] using an IBM/SP2 9076 located at UFSC facilities and on a Compaq cluster at the University of Sao Paulo LCCA Laboratory.

Results and discussion

Monomer electrochemistry Although a description of the electrochemistry of the monomer can be found elsewhere [3, 22], in particular the detailed assignment of the $Ru^{3+/2+}$ wave at −0.105 V vs Ag/Ag^+ (−0.18 V vs Fc/Fc^+), the $Ru^{4+/3+}$ process *trans*-$[RuCl_2(vpy)_4]^{+/2+}$ has not yet been published. It is relatively rare for the $Ru^{4+/3+}$ wave to appear within the solvent window for Ru pyridyl complexes unless donor ligands such as chloro [24] or phenolato [25] ligands are also present in the coordination sphere. On Pt, the wave consists of a partially reversible peak (Fig. 1) with $E^{0'}$=+1.475 V (ΔE_p=110 mV) vs Ag/Ag^+ (+1.40 V vs Fc/Fc^+). The irreversibility of the process is associated with the instability of the Ru^{4+} species, which is presumably easily hydrolyzed. The reduction of the ligand vinylpyridine takes place during two reduction waves: a first reduction wave observed at ca. E_{pc}=−1.5 V and a second one at ca. E_{pc}=−2.4 V vs Ag/Ag^+ [22]. They are much more cathodic than for vinylbpy or vinyl-tpy because there is less delocalization of the negative charge. There may also be a metal-based reduction in this highly cathodic region.

Electropolymerization

Effect of substrate To investigate the effect of the substrate material on electropolymerization, films were deposited by cyclic voltammetry onto Au, Pt, or glassy carbon (GC) elec-

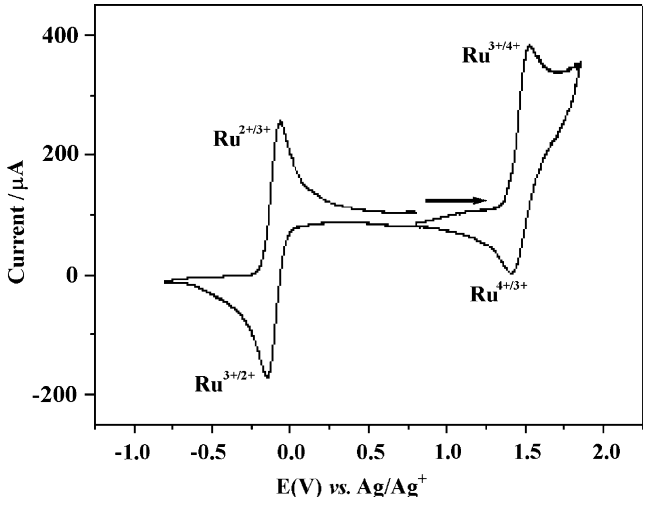

Fig. 1 Voltammetric profile of *trans*-$[RuCl_2(vpy)_4]$ complex (5 mmol dm^{-3} in CH_3CN/CH_2Cl_2 (3/2) at 50 mV s^{-1} on Pt)

trodes. The efficiency of polymerization was obtained by dividing the anodic charge of the $M^{3+/2+}$ reaction of the metallic center immobilized in the resulting polymeric film $\left(Q_a^{Ru(II)/Ru(III)}\right)$ by the total cathodic charge of the reductive polymerization $\left(Q_c^{poly}\right)$. This parameter, $\phi_{pol} = Q_a^{Ru(II)/Ru(III)} / Q_c^{poly}$ and in previous studies, [4] was found to be roughly six times greater on Au than that obtained for GC and twice that measured for polymerization on Pt (Table 1). Such dependence on the substrate could be associated with a variety of factors such as different heterogeneous rate parameters, adsorption or nucleation behavior, or adhesion properties. Both Au and Pt electrodes depicted excellent reproducibility regarding film deposition. The same situation was not observed for GC electrodes. Electrode preparation plays an important role in defining the reproducibility of the deposited films, as previously reported for the electropolymerization of other metallic complexes [3, 5, 22].

Effect of potential Electropolymerization was carried out at different potentials to study the effect of the polymerization potential on the characteristics of the films. The apparent surface coverage (Γ_{app}) and polymerization efficiency (ϕ_{pol}) promoted by each polymerization potential were monitored. Γ_{app} was calculated using $\Gamma_{app} = Q_a^{Ru(II)/Ru(III)} / nFA$ [26]. The results obtained from these analyses are listed in Table 2.

Although the values of ϕ_{pol} revealed an apparent maximum efficiency between −0.8 and −0.9 V vs Ag/Ag^+, Γ_{app} was very low at such potentials, suggesting the presence only of an adsorbed monolayer on the electrode instead of a polymeric film. According to the CV of the monomer in solution, three processes were observed between −0.80 and −2.6 V, at −0.8, −1.5, and −2.45 V vs Ag/Ag^+. Reduction at −1.5 and −2.45 V was attributed to the first and second waves of the ligand (vpy), respectively, confirming findings for similar complexes; for example, the reduction of the vinyl ligand in [Ru(trpy)(vpy)$_3$] occurs at −1.76 V [4, 5]. The process observed at −0.8 V, similar to that observed for a series of vinyl–bipyridine ruthenium complexes [4, 5], has traditionally been associated with an adsorption prewave reduction of the vpy ligand, but it could also be associated with a "prepolymerization prewave" during which the monomer is rapidly used up near the electrode by dimerization and polymerization follow-up reactions [27].

Both the polymerization efficiency and the apparent surface coverage significantly increased when polymerization took place at more cathodic potentials than that of the second reduction wave of vpy at −2.45 V [4]. At −2.9 V, the efficiency slightly decreased, but the value of Γ_{app} was similar to that obtained at −2.8 V vs Ag/Ag^+. It is believed that the solvent deteriorated at highly negative potentials. This contributed to the measured charge that therefore did not originate only from the polymerization reaction, thus accounting for the drop in ϕ_{pol}.

Table 1 Polymerization efficiency (ϕ_{pol}) of films deposited by CV between 0.7 and −2.0 V vs Ag/Ag^+ at 50 mV s^{-1}

Electrode	$\phi_{pol}\times 10^{-3}$	$\left(Q_c^{poly}\right)$(mC cm^{-2})	$\left(Q_a^{Ru(II)/Ru(III)}\right)$ (μC cm^{-2})
Au	2.82	35.00	98.83
Pt	1.08	316.00	342.70
GC	0.51	225.45	114.70

Film characterization by CV between −0.1 and 0.6 V vs SCE in 0.1 M $LiClO_4$ in CH_3CN at 100 mV s^{-1}

Table 2 Values of E_{pol}, Γ_{app}, and ϕ_{pol}. Films polymerized on Pt at fixed potential during 120 s

E_{pol} (V) vs Ag/Ag^+	$\Gamma_{app}\times 10^{-9}$ (mol cm^{-2})	$\phi_{pol}\times 10^{-3}$
−0.8	0.02	2.88
−0.9	0.09	11.61
−1.0	0.13	0.15
−1.7	0.20	0.13
−1.9	0.25	0.14
−2.4	0.35	0.13
−2.6	0.66	0.12
−2.7	3.42	2.06
−2.8	6.50	1.64
−2.9	6.36	0.97

EQCM

Experiments using a quartz crystal microbalance were carried out during the polymerization of *trans*-[$RuCl_2$(vpy)$_4$] to track the phenomena that took place during the process. Unfortunately, it was not possible to run experiments at potentials more negative than about −2.0 V due to instabilities. Typical current–potential, frequency–potential, charge–potential, and frequency–charge profiles are illustrated in Fig. 2. The cyclic voltammetry wave centered at −0.050 V shown in Fig 2a corresponded to the redox wave of the ruthenium metallic center ($Ru^{3+/2+}$). This was shifted slightly from that observed in the CV cell due to reference electrode differences. Those observed at −1.1 and −1.4 V corresponded to the prewave and vpy ligand reduction mentioned above. When interpreting the EQCM results, we use the familiar Sauerbrey equation [28]:

$$\Delta f = \Delta c_f \Delta m \tag{1}$$

where Δf is the change in frequency, c_f is the sensitivity factor and Δm is the mass change. Using $c_f = 0.232$ Hz cm^2 ng and an oscillating area of 0.205 cm^2, we expect that a frequency decrease of 1 kHz corresponds to a mass change of 883 ng on the oscillating area. The application of this equation assumes that the adhered mass forms a rigid film on the oscillating surface. In practice, this is met

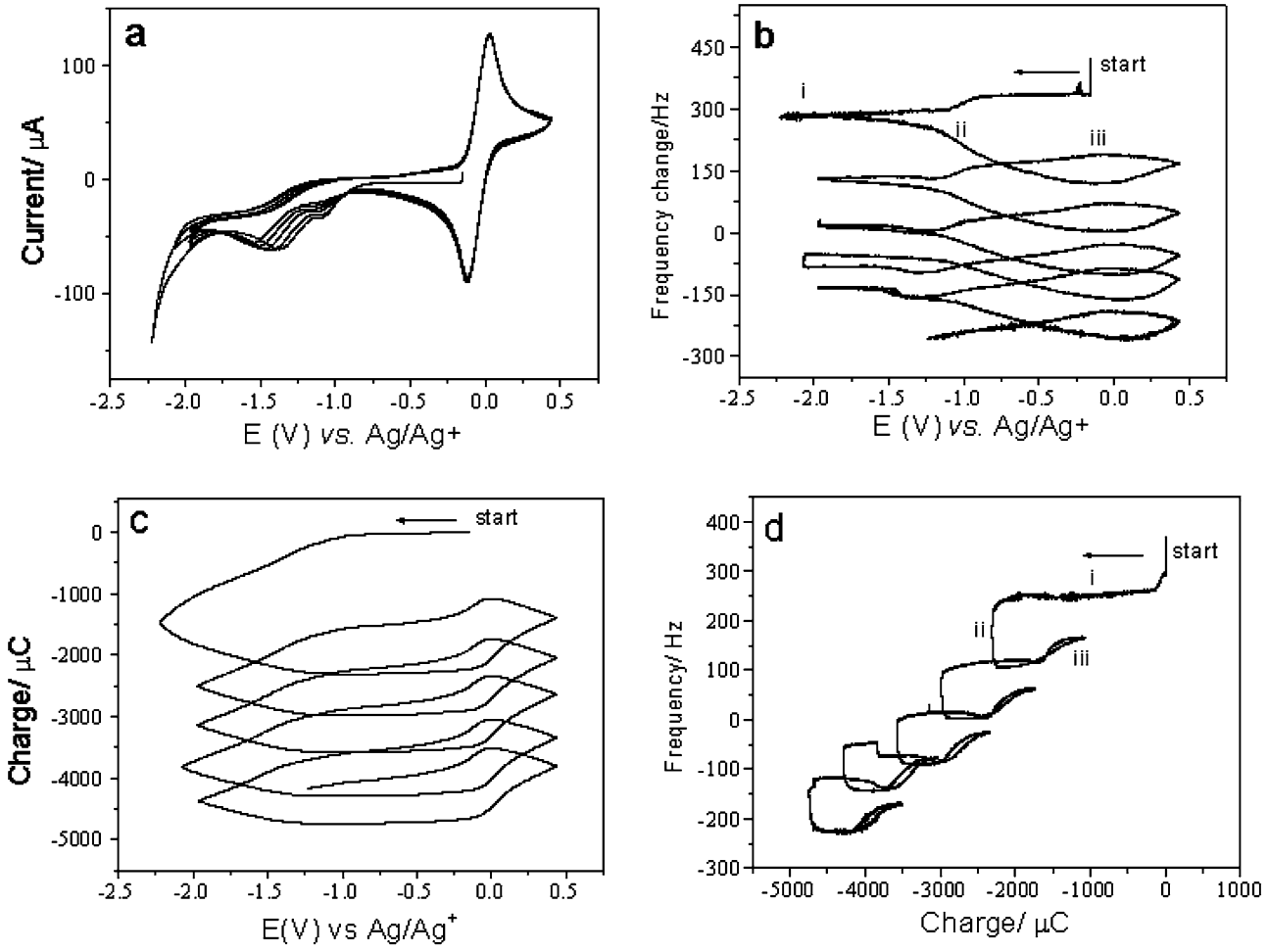

Fig. 2 **a** CV. **b** Frequency/potential profile. **c** Charge/potential profile. **d** Frequency/charge profile. Obtained upon electropolymerization of poly-{*trans* $[RuCl_2(vpy)_4]$}$_n$ on Au at 50 mV s^{-1}

by limiting the film thickness. Assuming a density of approximately 1 g cm^{-3}, we estimate that 1 kHz corresponds to a thickness of about 0.04 μm. Most of the films studied were well below this thickness. Furthermore, a linear change with frequency with the charge during polymerization gives strong evidence that the film is rigidly coupled to the electrode [29]. As shown in Fig. 2b, during the first cycle, the frequency decreased suddenly by about 70 Hz at −0.9 V and continued decreasing at a slower rate throughout the cathodic scan and along with the most of the anodic scan. When the voltammetric wave was scanning over the $Ru^{3+/2+}$, the trace became a hysteresis loop. Subsequent cycles repeated the pattern but at ever lower frequencies, reflecting the steady increase in mass due to film growth. There was no evidence for desorption processes as observed in the microgravimetry during the reduction of $[Ru(bpy)_2Cl_2(CO)_2]$ complexes [30]. Instead, the traces are reminiscent of those reported for the electropolymerization of $[Ni(vinylterpy)_2]^{2+}$, which, like other vtpy and vbpy complexes, appears to electrodeposit the films at potentials well above those at which the ligand is reduced [31, 32]. Thus, three distinct regions characterized the potential cycle investigated (Fig. 2a–c): polymerization (region marked i), movement of anions and/or solvent (region ii), and to and from the film and corresponding redox of the metallic center (region iii) (Fig. 2b).

The charge–potential plot confirmed the coupling of the mass changes in the 0 to +0.5 V region with the Ru redox processes. Oxidation of the Ru in the film leads to an increase in mass due to the ingress of anions and associated solvent molecules [33]. Curiously, the largest changes in frequency occurred when no reactions took place between −1.0 and 0.0 V during the reverse potential scan (Fig. 2b). The decoupling of this mass change from any passage of charge is seen clearly in the dramatic ca. 100 Hz vertical steps in Fig. 2d. This indicated that the frequency variation observed in this potential range was associated with a nonfaradaic process, such as the penetration of ions and/or solvent into the film or, alternatively, modifications in the solvation and/or film morphology. However, the mass changes expected for these processes are much too small to account for the observed changes. Instead, we propose that the "vertical" frequency steps in Fig. 2d are due to the deposition of oligomeric species from solution. Similar EQCM features ascribed to oligomer deposition have been observed during the electropolymerization of thiophene derivatives [34]. This deposition is induced by either

potential-independent or potential-dependent adsorption or even reoxidation of the oligomers as long as their lengths are diverse and their potentials span a wide range of potential, so that the charge passed is small and spread out over a wide potential range. Finally, despite the deposition of extra mass due to the oligomers, there seems to be a lower increase than expected in the mass changes accompanying the $Ru^{3+/2+}$ process. This might indicate that the deposited oligomers are not as electroactive as the film deposited at potentials < −0.9 V. The region between −0.9 V and the switching potential actually corresponds to the steady deposition of insoluble polymer. The efficiency of this process may be obtained [30, 35] from the slopes of the frequency–charge plot (Fig. 2d) which yields a slope of 2.5×10^{-5} g C^{-1} (the slope was obtained, taking as reference points the upper left corners of the squares in Fig. 2d). Using Faraday's Law, the mass of polymer produced, m, is given by M_rQ/nF where M_r is the relative molar mass of the monomer unit. Assuming the theoretical 100% polymer deposition efficiency (M_r=592.5) and that one electron or less is needed to initiate polymerization, the slope should be at least 6×10^{-3} g C^{-1}. Clearly, the observed slope is much lower. While it is possible that some of the inefficiency may be due to faradaic side reactions, the small size of the background currents at these modest cathodic potentials is not enough to account for this. Instead, we believe that most of the charge is used to produce soluble oligomer and/or vinyl anionic radicals which decay by follow-up reactions with trace water, for example, rather than polymerizing (though we note that deliberate addition of water does not affect the polymerization). Finally, by multiplying by F/M_r, it is also possible to calculate from the slope of the frequency–charge plot an observed polymer efficiency ϕ_{pol} of 4.1×10^{-3}, not too far from the value obtained for gold in Table 1 using coulometry. Due to the adsorption of the oligomers during the anodic potential sweep, the "global" polymerization efficiency in the cyclic voltammetry experiment as calculated from the slope of the line tangent to the traces in Fig. 2d is 1.15×10^{-3} g C^{-1}, significantly higher than the rate in the region below −0.9 V and closer to the theoretical value above.

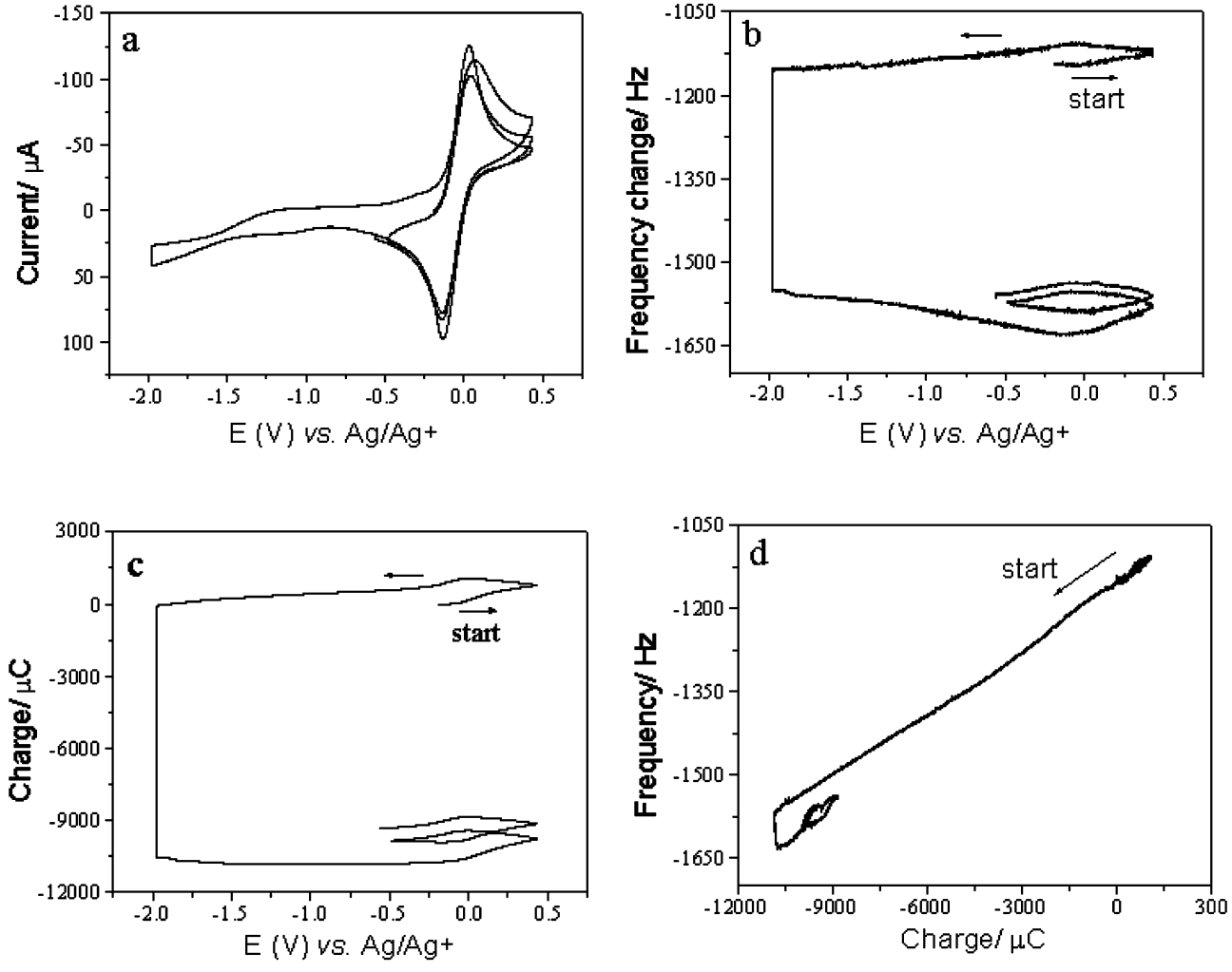

Fig. 3 **a** CV. **b** Frequency/potential profile. **c** Charge/potential profile. **d** Frequency/charge profile. Obtained upon electropolymerization of poly-{*trans* $[RuCl_2(vpy)_4]$}$_n$ on Au at 50 mV s^{-1}. Potential set to −2.0 V vs Ag/Ag^+ during 345 s

Table 3 Calculated (HF/6-31G (d,p), scaled and experimental [40] wavenumbers of the ligand 4-vinylpyridine (vpy) and experimental wavenumbers of the solid complex [36] (cm^{-1})

vpy (calculated)	vpy (scaled)	vpy (experimental) [40]	Solid complex (experimental) [36]	Assignment
1,867	1,640	1,635	1,626	ν(C=C) vinylic
1,811	1,592	1,590	1,604	ν_{8a}
1,350	1,197	1,236	1,219	ν_{9a}
1,329	1,179	1,217	1,200	ν_{13} [ν(C–X) + β(CH) ring]
1,180	1,051	1,067	1,057	β(CH)
1,131	1,009	991	1,032	ρ(CH_2)vinyl
1,091	975	987	1,013	ν_{12} (trigonal ring breathing)
849	767	787	799	ν_1 + ρ(CH_2)vinyl + β(CH)ring
–	–	–	258	ν(Ru–N)

However, we do not believe this extra material is electroactive because the coulometrically determined polymer efficiencies are more consistent with the polymerization rate in the −0.9 to −2.0 V region as shown above.

Subsequent polymerization at fixed potential (−1.6 or −2.0 V) for a few seconds in the same experiment (i.e., on the same films and in the same solution, to minimize changes in the experimental conditions and to conserve quartz crystals) resulted in similar behavior to that observed during cyclic voltammetry (Fig. 3). At both potentials, the frequency rapidly decreased immediately after the potential was set. The frequency–potential plot shows (Fig. 3b) that the mass changes in the $Ru^{3+/2+}$ redox range are considerably greater after polymerization, as expected after the growth of a thicker electroactive film. For films produced at fixed potential, the frequency decreased linearly and steadily at rates of 1.50 and 1.32 ng s^{-1}, for −1.6 and −2.0 V, respectively, after deposition for 345 s. The corresponding efficiencies from the slopes of the frequency–charge plots (such as Fig. 3d for −2.0 V) were 4.0×10^{-5} and 3.5×10^{-5} g C^{-1}. These polymerization efficiencies are significantly lower than those observed for similar complexes of the type $[M(v\text{–}tpy)_2]^{2+}$, (M=Fe, Ru, Os), which were approximately 4×10^{-4} g C^{-1} at −1.1 V [27]. This probably reflects the greater stability of the more delocalized vinyl-terpy ligand anion radicals. If we convert our observed polymerization efficiencies to faradaic efficiencies, by multiplying by F/M_r, these translate to 6.5 and 5.7×10^{-3}. Compared to the values shown earlier in Table 2, these are a factor of 40 too high. The discrepancy probably derives from the use of gold rather than platinum electrodes because gold appears to favor polymerization under CV conditions (Table 1).

Comparing the polymer efficiency rates for the two techniques, it could be seen that films grew a little slower by cyclic voltammetry if only the potential range below −0.9 V was considered. This is unsurprising, as the cycle obviously does not sample the extreme cathodic potentials as much as a potentiostatic experiment does. Moreover, the growth rate of films deposited at −2.0 V was somewhat lower than that obtained at −1.6 V, contrary to what was expected. More cathodic potentials should favor the reduction of the vinyl group, hence, accelerate the polymerization rate. It is possible, as Kvarnström et al. [27] have pointed out for the electropolymerization of poly (*p*-phenylene), that more extreme potentials encourage the multielectron reduction and growth of soluble oligomers. This uses up monomer which would otherwise form polymer on the electrode surface.

Results from the EQCM experiments indicated that polymerization occurred only in the cathodic region below −0.9 V and is presumably initiated by the reduction of the ligand vpy. Above −0.9 V, there was a large increase in mass on the surface of the electrode from the deposition of oligomers which may be less electroactive than the underlying polymer.

Raman spectroscopy

The Raman spectrum of the solid complex was already reported by Bandeira et al. [36]. In the range between 1,000 and 1,650 cm^{-1}, the Raman spectrum of the solid complex showed several bands assigned to pyridine ring and vinyl

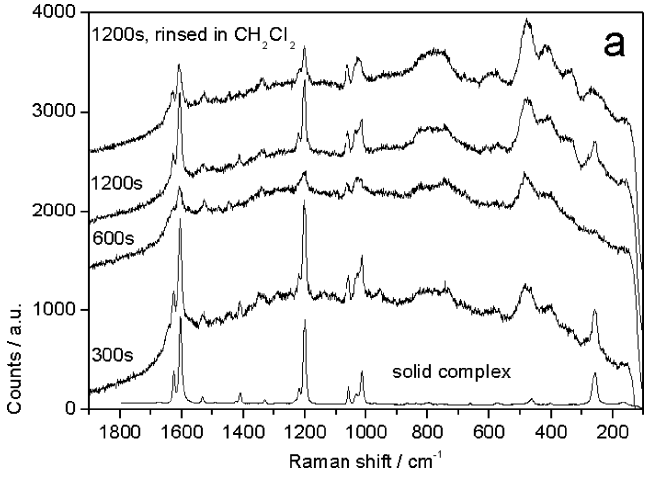

Fig. 4 Raman spectra of poly-{*trans* $[RuCl_2(vpy)_4]\}_n$ film on Au in polymerization (fixed potential) at −0.7 V vs Ag/Ag^+

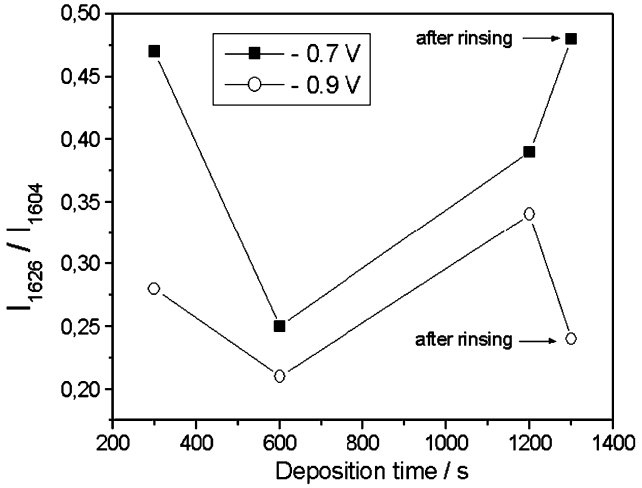

Fig. 5 Time deposition evolution of the intensity ratio between the bands at 1,626 and 1,604 cm^{-1}, for the potential −0.7 and 0.9 V

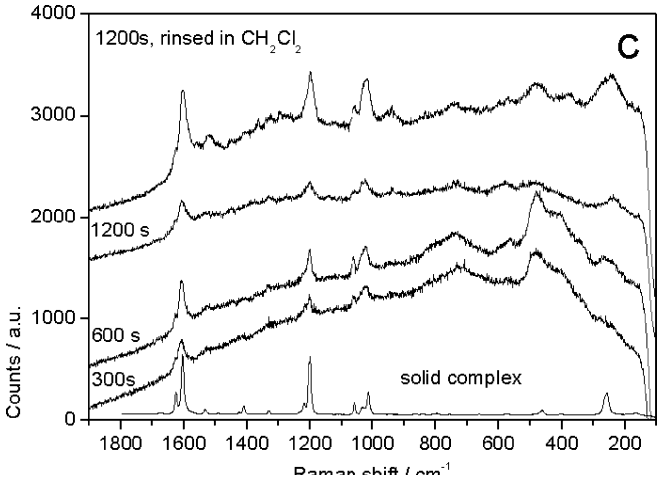

Fig. 7 Raman spectra of poly-{*trans* $[RuCl_2(vpy)_4]\}_n$ film on Au in polymerization (fixed potential) at −1.6 V vs Ag/Ag^+

group modes. According to previous studies on similar systems, there is a great mixing of ring vibrational modes and also between ring and substituent modes [37]. A medium band at ca. 1,626 cm^{-1} was assigned to ν(C=C), from the unreacted vinyl groups. In the low wave number region, a medium band at ca. 258 cm^{-1} was assigned to ν(Ru–N) [38–40]. It is assumed that the band positions of the complex and free ligand are nearly identical, as noticed for other complexes containing vpy by Topacli and Bayari [39]. An assignment of the main ligand modes based on ab initio calculations [HF/6-31G(d,p)] is given in Table 3. The calculated frequencies were scaled according to the procedure outlined by Sala et al. [37]. Wilson numbering was used in the vibrational mode description of the pyridine ring modes. Experimental wave numbers for the free ligand and the solid complex taken from the literature are also presented [36, 40].

Raman spectra of films grown onto Au electrodes at different potentials revealed some changes compared to the spectrum of the monomer complex. One of the main differences was the variation of the intensity ratio between bands at 1,604 (ν_{8a}) and ca. 1,626 cm^{-1} (νC=C), which was an indication of the degree of polymerization, as established by Noda and Sala [41] for styrene and its oligomers. To compare the change in the spectra, the Raman spectrum of the solid complex was reproduced at the bottom of each group of spectra. The absolute intensities of each spectrum were preserved in the graphs.

At −0.7 V (Fig. 4), the initial spectrum (t=300 s) still revealed some characteristics of the monomer complex: the presence of the band at 1,626 cm^{-1} and the band at 1,032 cm^{-1}, weaker than the band at 1,013 cm^{-1}. However, as the band at 1,626 cm^{-1} has lower intensity ratio (in relation to the band at 1,604 cm^{-1}) than the same band in the monomer, these features indicate an initial polymerization of the complex. The presence of broad bands in the 500 to 800 cm^{-1} range, attributed to possible ruthenium oxides formed by the complex decomposition, was also noted [42]. Increasing the deposition time, the bands at ca.

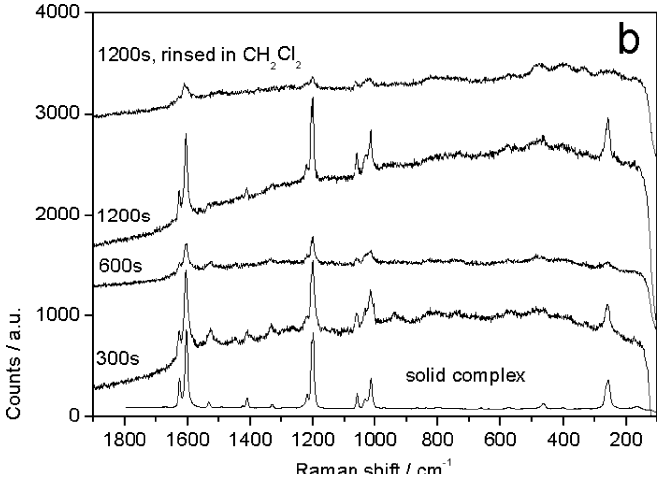

Fig. 6 Raman spectra of poly-{*trans* $[RuCl_2(vpy)_4]\}_n$ film on Au in polymerization (fixed potential) at −0.9 V vs Ag/Ag^+

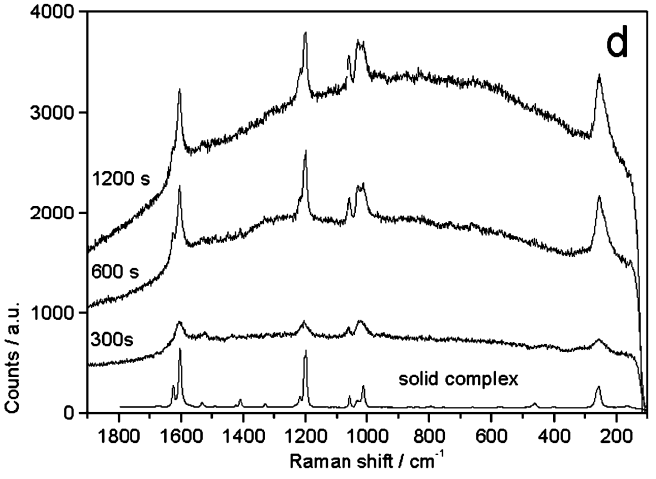

Fig. 8 Raman spectra of poly-{*trans* $[RuCl_2(vpy)_4]\}_n$ film on Au in polymerization (fixed potential) at −2.9 V vs Ag/Ag^+

1,032, 1,200, and 1,604 cm^{-1}, characteristic of the presence of a film, slightly decreased. A reasonable explanation for this comes from the heterogeneities of the coated surface characterized by both rich and depleted regions of polymerized material. As a result of the high spatial resolution typical of the Raman microscope and the difficulty to keep it focused in the same spot for long periods of time, a random variation in the absolute intensity of bands is expected [43].

Assuming that the intensity ratio between bands at ca. 1,626 [ν(C=C) vinylic] and 1,604 cm^{-1} (ring) was an indication of the degree of film polymerization, a decrease in intensity of the band at ca. 1,626 cm^{-1} for t=600 s suggested the formation of a longer chain or more highly cross-linked polymer. Subsequently, at t=1,200 s, there was an increase in the relative intensity of the band at 1,626 cm^{-1} (see the graph in the Fig. 5). This could be explained by the formation of shorter, soluble chains in the outer layers of the film (away from the electrode), indicating a reduction in the degree of polymerization or cross-linking. Rinsing the film with dichloromethane resulted in a Raman pattern typical of partial polymerization, as confirmed by the presence of the vinylic double bond stretching band. The relative intensification of the band at ca. 500 cm^{-1} suggested that rinsing with CH_2Cl_2 solubilized a substantial fraction of the film.

A decrease in intensity of the low-frequency bands (except for the band at ca. 258 cm^{-1}), probably related to a decrease in the formation of ruthenium oxide, could be noticed when comparing the spectra obtained during polymerization at −0.9 V (Fig. 6) and at −0.7 V. The relative intensity of the band at ca. 1,626 cm^{-1} also varied with time in a similar way to that observed at −0.7 V (see the graph in Fig. 5). However, the relative intensity of the band at ca. 1,626 cm^{-1} in the film rinsed with CH_2Cl_2 decreased from −0.7 to −0.9 V, indicating a higher degree of polymerization at more negative potentials.

Films grown at −1.6 V (Fig. 7) showed low intensity bands at ca. 1,626 cm^{-1} in every spectrum gathered, suggesting a high degree of polymerization or cross-linking at this much more cathodic polymerization potential. Similarly, it has been shown by spectroelectrochemical techniques that a 255-nm band characteristic of the vinyl ligand completely disappears at −1.8 V and does not recover [44]. The band at ca. 258 cm^{-1} (νRu–N) was broader than the corresponding ones in the −0.7 and −0.9 V spectra. As the first reduction wave of the ligand was located at ca. −1.4 V, it became clear that the formation of a film with high degree of polymerization or cross-linking was only possible at cathodic potentials beyond −1.4 V vs Ag/Ag^{+}. It is believed that the Ru–N bond strength could have been modified by the electronic redistribution in the pyridinic ring associated with complete polymerization of all the vinyl groups. This might be responsible for the change in frequency observed for the band at ca. 258 cm^{-1}.

Finally, high degrees of polymerization or cross-linking were characteristics of the entire process at −2.9 V (Fig. 8), as suggested by the low relative intensity of the band at ca. 1,626 cm^{-1}. No broad bands were observed in the low-frequency region, indicating that at this potential no ruthenium oxide was formed. The intensity of all bands increased with deposition time, suggesting film thickening. Only the ν(Ru–N) band was observed in the low-frequency range, positioned at ca. 258 cm^{-1}. Polymerization was probably quite fast at this potential and no intermediate species were formed or detected. It could be concluded that films grown at potentials lower than that of the first reduction wave of vpy showed partially reacted vinyl groups associated with lightly cross-linked polymer or oligomers in the beginning of polymerization. This was not observed at more cathodic potentials. The Raman data helps to confirm that only small amounts of polymeric material, some of which is soluble in rinsing solvent, and unreacted monomer are deposited on the electrode at potentials close to the −0.8 V "prewave", and that this material contains a substantial fraction of unreacted vinyl groups. Substantial amounts of polymer are deposited at more negative potentials (−1.6 V) with evidence of more fully reacted vinyl groups. This is in good agreement with the results of EQCM (steady polymer deposition at potentials <−1.0 V). The interesting additional information provided by the Raman spectroscopic data is that the films deposited at both −1.4 and −2.0 V have few unreacted vinyl groups and may therefore be regarded as fully cross-linked.

Conclusions

Polymerization efficiency and EQCM measurements, as well as Raman spectroscopy, confirmed that polymer formation is observed at potentials much more positive than that of the first reduction wave of the vpy ligand. For short polymerization times, the greatest polymerization efficiency on Pt was obtained at extremely cathodic potentials. EQCM data indicated that reasonable efficiencies for deposition of poly{*trans*-[$RuCl_2(vpy)_4$]} films were measurable on gold at cathodic potentials between −0.9 and −2.0 V. Potential cycling also led to deposition of substantial amounts of oligomeric material near −0.9 V, but this material seemed to be less electroactive. Raman spectra revealed that the structure of the films was similar to that of the monomer and confirmed the presence of adsorbed monomer and only small amounts of film unless the potential was more cathodic than −0.9 V. The Raman spectra also indicated that potentials more cathodic than −1.6 V were required before all the vinyl groups had reacted in the film.

Acknowledgements The authors are grateful to Laboratório de Espectroscopia Molecular (LEM-IQUSP) for the use of the Raman equipment (Renishaw Raman System 3000). LKN acknowledges CAPES/ProDoc for the grant, NSG acknowledges CNPq Edital Universal 01/2002, and MCEB acknowledges CAPES-Brazilian Research Council for financial support.

References

1. Paula MMS, Franco CV (1996) J Coord Chem 40:71
2. Paula MMS, Franco CV, Prates PB, Moraes Jr VN (1997) Synth Met 90:81
3. Paula MMS, Franco CV, Mocellin F, Moraes Jr VN (1998) J Mater Chem 8:2049
4. Calvert JM, Schmehl RH, Sullivan B.P, Facci JS, Meyer TJ, Murray RW (1983) Inorg Chem 22:2151
5. Denesevich P, Abruña HD, Leidner CR., Meyer TJ, Murray RW (1982) Inorg Chem 21:2153
6. Bandeira MCE, Prochnow FD, Costa I, Franco CV (2001) Key Eng Mater 189–191:673
7. Bandeira MCE, Prochnow FD, Costa I, Franco CV (1999) J Corros Sci Eng 2:paper 4. http://www2.umist.ac.uk/corrosion/JCSE/
8. Bandeira MCE, Prochnow FD, Costa I, Franco CV (1999) Brazilian Patent MU 7900518-7, Brazil
9. Sobral AVC, Ristow Jr W, Domenech SC, Franco CV (2000) J Solid State Electrochem 4:417
10. Foster RJ, Vos JG (1991) J Chem Soc Faraday Trans 87:1863
11. Doherty AP, Foster RJ, Smyth MR, Vos JG (1992) Anal Chem 64:572
12. Doherty AP, Vos JG (1992) J Chem Soc Faraday Trans 88:2903
13. Doherty AP, Stanley MA, Leech D, Vos JG (1996) Anal Chim Acta 319:111
14. Araki K, Angnes L, Azevedo CMN, Toma HE (1995) J Electroanal Chem 397:205
15. Gorski W, Aspinwall CA, Lakey JRT, Kennedy RT (1997) J Electroanal Chem 425:191
16. Azevedo CMN, Araki K, Toma HE, Angnes L (1999) Anal Chim Acta 387:175
17. Mccarley RL, Thomas RE, Irene EA, Murray RW (1990) J Electrochem Soc 137:1485
18. Brown NMD, You HX, Forster RJ, Vos JG (1991) J Mater Chem 1:517
19. Pasa-Creczynski TB, Bonetti VR, Beirith A, Ckless K et al (2001) J Inorg Biochem 86:587
20. Elliott MC, Baldy JC, Nuwaysir LM, Wilkins CL (1990) Inorg Chem 29:389
21. Bandeira MCE (2001) Ph.D. thesis. Materials Science and Engineering, UFSC Florianópolis, SC-Brazil
22. Paula MMS (1999) Ph.D. thesis. Materials Science and Engineering, UFSC Florianópolis, SC-Brazil
23. Frisch MJ, Trucks GW, Schlegel HB, Scuseria GE et al (1998) Gaussian, Wallingford, CT
24. Kojima T, Amano T, Ishii Y, Ohba M, Okaue Y, Matsuda Y (1998) Inorg Chem 37:4076
25. Holligan BM, Jeffery JC, Norgett MK, Schatz E, Ward MD (1992) J Chem Soc Dalton Trans 23:3345
26. Bard AJ, Faulkner LR (2001) Electrochemical methods—fundamentals and applications, 2nd edn. Wiley, NY, USA, p 580
27. Kvarnström C, Bilger R, Ivaska A, Heinze J (1998) Electrochim Acta 43:355
28. Sauerbrey H (1959) Z Phys 155:227
29. Baker CK, Reynolds JR (1988) J Electroanal Chem 307:251
30. Myllynen S, Wasberg M, Eskelinen E, Haukka M, Pakkanen TT (2001) J Electroanal Chem 506:115
31. Takada K, Storrier GD, Pariente F, Abrunã H (1998) J Phys Chem B 102:1387
32. Storrier GD, Takad K, Abrunã H (1999) Inorg Chem 38:559
33. Varela H, Malta M, Torresi RM (2000) Quím Nova 23:664
34. (a) Dini D, Decker F, Zotti G (1998) Electrochem Sol State Lett 1:217 (b) Skompska M (2000) Electrochim Acta 45:3841 (c) Zhao ZS, Pickup PG (1994) J Chem Soc Faraday Trans 90:3097
35. Snyder SR, White HS (1995) J Phys Chem 99:5626
36. Bandeira MCE, Prochnow FD, Noda LK, Gonçalves NS (2004) J Solid State Electrochem 8(4):244
37. Sala O, Gonçalves NS, Noda LK (2001) J Mol Struct 565–566:411
38. Paula MMS, Konzen M, Seifriz I, Gonçalves NS, Spoganickz B, Franco CV (1999) J Bioinorg Chem 76(3–4):153
39. Topacli A, Bayari S (2001) J Mol Struct 595:93
40. Bayari S, Yurdakul S (2000) Spectrosc Lett 33(4):475
41. Noda LK, Sala O (2000) Spectrochim Acta A 56:145
42. Liu HL, Yoon S, Cooper SL, Cao G, Crow JE (1999) Phys Rev B Condens Matter 60(10):R6980
43. Santos PS, Gonçalves NS (2001) J Mol Struct 570(1–3):75
44. Paulson SC, Elliott CM (1996) Anal Chem 68:1711